Applied Catalysis B: Environmental 174–175 (2015) 383–394

Contents lists available at ScienceDirect

Applied Catalysis B: Environmental

journal homepage: www.elsevier.com/locate/apcatb

Deoxygenation and cracking of free fatty acids over acidic catalysts by single step conversion for the production of diesel fuel and fuel blends

Konstantin Hengst, Matthias Arend, Rebecca Pfützenreuter, Wolfgang F. Hoelderich*

Formerly: Department of Chemical Technology and Heterogeneous Catalysis, RWTH Aachen University, Worringerweg 1, D-52074 Aachen, Germany

ARTICLE INFO

Article history:
Received 11 November 2014
Received in revised form 1 March 2015
Accepted 5 March 2015
Available online 13 March 2015

The paper is devoted to the 75th birthday of Prof. Dr. Jacques Vedrine and in recognition of his tremendous work for the catalysis community and Applied Catalysis, Elsevier. This paper is also devoted to the 70th birthday of Dr. John Armor and in recognition of his outstanding work and contributions to the catalysis community.

Keywords:
Biofuel
Deoxygenation
Cracking
Oleic acid
Aluminium oxide
Zeolite
Silica aluminates

ABSTRACT

Gas phase deoxygenation of oleic acid was accomplished over palladium containing acidic catalysts under solvent-free conditions. Aluminum oxide catalysts were prepared out of three different boehmite precursors by calcination at different temperatures between 500 °C and 1100 °C forming different aluminum oxide phases. All catalysts were impregnated with 1 wt.% palladium and subsequently tested for their deoxygenation performance either batch wise in autoclaves or continuously in a fixed bed plug flow reactor or in a trickle bed reactor. Conversion of oleic acid and selectivity to the desired diesel-like C17 hydrocarbons heptadecane and heptadecenes were studied with the best aluminum oxide found in the catalyst screening at different reaction temperatures, catalyst amounts and palladium amounts on the catalyst. Using boehmite found as best alumina precursor, different mixtures of such aluminum oxide with zeolites were prepared in order to increase the catalyst acidity and thus the deoxygenation performance. The optimum reaction conditions found for aluminum oxide catalysts were applied for the screening of these composite catalysts. Using the best composite catalyst, the effect of hydrogen dilution with nitrogen, the addition of water and catalyst regeneration by thermal treatment was tested. In addition catalyst containing silica aluminates doped with 1 wt.-% Pd were prepared and tested for their catalytic activity in deoxygenation and cracking of free fatty acids. Some reactions were conducted under elevated hydrogen pressure. The catalysts were characterized by nitrogen adsorption isotherms (BET), temperature programmed desorption of ammonia (TPD), X-ray powder diffraction (XRD), thermo gravimetric analysis (TGA) and field emission scanning electron microscopy (FESEM).

1. Introduction

Increasing anthropogenic CO_2 in the atmosphere and diminishing fossil energy resources have generated a great interest in renewable biofuels. 1st generation biodiesel derived by transesterification of fats and oils into fatty acid methyl esters (FAME) is well known, industrially applied and still subject of research [1,2]. FAME has however many drawbacks, such as higher boiling points of C16–C18 fractions, higher cloud point and higher viscosity compared with petroleum derived diesel [3]. These facts cause problems in the conventional diesel engines. Therefore, in the European Union FAME is usually blended with conventional diesel to provide a partially renewable diesel [4].

To prevent the undesired formation of surfactants, the typically homogeneously catalyzed process requires a high purity of the triglycerides and competes with the human food chain [5]. Different processes were developed in order to use non-edible raw materials. Fuels obtained from these feedstocks are generally called 2nd generation biofuels [6] consisting of hydrocarbons with similar properties as petroleum derived fuels. Feedstocks of these fuels are all non-edible biomasses, such as cellulosic material, woody-biomass, crop residues or algaes [7,8], as well as free fatty acids which are generally removed from oils and fats. However, 2nd-generation biofuels also include traditional feedstocks like edible oils and fats, even though these obtained fuels only consist of conventional diesel-like hydrocarbons [9,10]. The first commercial process producing biodiesel from waste materials is the NExBTL process (Neste Oil). The properties of the biodiesel are superior to fossil based diesel due to the high cetane number which makes the NExBTL biodiesel also an excellent blend [11]. Also the H-oil process (Petrobas) [12], Green Diesel (UOP/Honeywell) [13] and SunDiesel (Choren/Volkswagen) [14] are industrialized biomass-to-liquids (BTL) processes which are considered as 2nd -generation biofuels. Generally, in BTL processes, carbonaceous material/biomass is

* Corresponding author. Tel.: +49 623362442.
E-mail address: hoelderich@rwth-aachen.de (W.F. Hoelderich).

http://dx.doi.org/10.1016/j.apcatb.2015.03.009
0926-3373/

gasified in a first step at elevated temperatures with or without oxygen. The gasification includes the conversion processes partial oxidation and steam gasification and results generally in syngas [15]. The obtained syngas is subsequently used in Fischer–Tropsch (FT) synthesis to produce liquid fuels [16] or in the production of methanol which is afterwards converted either to gasoline (MTG-process) [17] or to olefins (MTO-process) [18]. The molecule breakdown and the consecutive build-up of hydrocarbons in FT or MTG result in the desired biomass derived fuels. However, another approach to obtain biomass derived fuels is the selective defunctionalization of biomass and biomass platform molecules under perpetuation of the nature built hydrocarbon framework which avoid the energy intensive gasification and FT synthesis. In recent years, intensive research was carried out in the field of converting triglycerides and their derivates into hydrocarbons. Two different types of metal supported catalysts are generally described in the literature for the oxygen removal from biomass feedstocks: first sulfided transition metal catalysts which are widely used as hydrotreating catalysts in petroleum industry, such as NiS/NiMo/γ-Al_2O_3 and CoMo/γ-Al_2O_3 [19–22] and second supported noble metal catalysts [23–30].

Snåre et al. tested various metals such as Ni, NiMo, Ru, Pd, Pd/Pt, Pt, Ir, Os and Rh on different supports (metal oxides and charcoal) in liquid phase reactions in order to determine their deoxygenation performance. Pd supported on carbon was found as the best catalyst [23]. Further investigations with Pd/C catalysts were mostly conducted in liquid phase using different solvents and under pressure in semi-batch autoclaves [24–26].

Immer et al. reported about the reaction pathways in liquid-phase deoxygenation of stearic acid (SA), oleic acid (OA) and linoleic acid. OA was deoxygenated in hydrogen atmosphere by sequential hydrogenation (1.1) and decarboxylation (1.2) whereas decarbonylation (2) occurred preferably in inert He atmosphere at substantially lower reaction rates.

$$C_{17}H_{33}COOH + H_2 \rightarrow C_{17}H_{35}COOH \quad (1.1)$$

$$C_{17}H_{35}COOH \rightarrow CO_2 + n\text{-}C_{17}H_{36} \quad (1.2)$$

$$C_{17}H_{33}COOH \rightarrow CO + H_2O + C_{17}H_{32} \quad (2)$$

Additionally, catalyst stability was enhanced in a 10 vol.-% H_2 (in He) atmosphere, probably thereby avoiding the formation of unsaturated hydrocarbon products adsorbed on the catalyst surface blocking the active centers and preventing further reactions [27].

Snåre et al. conducted liquid phase deoxygenation experiments in a continuous flow reactor under Ar atmosphere and solvent free conditions using a Pd/C catalyst. The main product was stearic acid, whereas the formation of hydrocarbons, mainly olefins and aromatics, were reported to be below 10 mol.-% [28].

Lestari et al. reported about the continuous deoxygenation of neat stearic acid in liquid phase over Pd catalyst supported on mesoporous carbon (Sibunit). A stable stearic acid conversion of about 15% was achieved with *n*-heptadecane as the main product. Based on continuous gas phase analysis, it was suggested that CO is formed by decarbonylation of stearic acid and reverse water-gas shift reaction out of CO_2 and H_2 [29].

Recently, we reported about solvent free gas-phase deoxygenation of OA over Pd/C catalyst. [30]. At high reaction temperatures of 380 °C, due to the high boiling point of OA, stearic acid was found as the major product and the highest obtained C17 selectivity was 28.5 mol%. Rather heavy coking of the Pd/C catalyst was assumed to result in a 99% loss of surface area. The formation of heptadecane in the absence of hydrogen showed that oleic acid deoxygenation was possible in an inert atmosphere probably by decarbonylation [30].

Besides the aforementioned metal supported catalysts, zeolites were also tested for valorizing vegetable oils into biofuels. A rather unselective deoxygenation was mainly achieved without hydrogen and resulted in a wide variety of products, such as aromatics, naphthenes, *n*- and *iso*-alkanes. Main products of acidic catalyzed cracking of vegetable oils were hydrocarbon gases (C_3–C_6), so-called organic liquid products (OLP) consisting of aliphatic hydrocarbons with traces of oxygenates and coke [31,32]. Usually, OLP consist of a gasoline fraction (C3–C5) which is desired for potential bio fuel applications. Besides cracking of pure vegetable oils or glycerol also co-feeding of vegetable oils or glycerol to conventional FCC feedstock was investigated [33,34]. Among zeolites, H–ZSM5 was found as the best catalyst for upgrading of vegetable oils and thus has been the most extensively investigated zeolite for the cracking of triglycerides [35,36]. Katikaneni et al. compared H–ZSM5 and potassium impregnated ZSM5 (K–ZSM5) and found that the latter resulted in a lower yield of hydrocarbons, particularly aromatics due to much lower density of strong Brønsted acidic sites. It was therefore concluded that the catalyst acidity is of major importance for the aromatization, which was considered as a consecutive reaction of the deoxygenation. However, it did not affect the initial deoxygenation [37].

The addition of steam was investigated by Čejka and Minetova who found thereby a diminished formation of aromatics by up to 20 wt.-%. It was proposed that hydride transfer was suppressed in the presence of steam. By the addition of steam the catalyst lifetime was extended, too. That was explained by possible competitive adsorption of water and coke molecules on the catalyst surface. Finally, the addition of steam resulted in an increased formation of gaseous products of up to 34 wt.-% of the feeding mass [38].

The conversion of used palm oil was enhanced by 20 wt.-% at 400 °C in presence composites of H–ZSM5 and MCM-41 in comparison with pure H–ZSM5 catalysts. However, if fatty acids alone were used as feedstock, conversion was only slightly improved. It was concluded, that the increased conversion was caused by reduced diffusion hindrances [39]. Neat mesoporous material showed significantly lower conversion due to their lower density and strength of acidic sites. The highest overall gasoline yield of 44 wt.-% was achieved over H–ZSM5/MCM-41 composites, containing 10–30 wt.-% mesoporous phase [40].

Amorphous silica–alumina catalysts were the first cracking catalysts used in petrochemical industry [41]. Silica–aluminates with a low content of aluminum have generally small pore volume, a high surface area and are less active then silica–aluminates with high aluminum content. In comparison with aluminum oxides, the silica–aluminates are strongly Brønsted acidic. Experiments showed that the most acidic catalyst is obtained with an Al_2O_3 content of 30 wt.-%. This Brønsted acidity is necessary for catalytic cracking reactions of long chain hydrocarbons accompanied by isomerization, polymerization and aromatization reactions [42,43].

The aim of this work is to study the hydrodeoxygenation of unsaturated OA over Pd impregnated acidic alumina, alumina/zeolite and silica alumina containing catalysts and furthermore the catalytic hydrogenation and decarboxylation of fatty acids in order to synthesize suitable fuels or fuel blending products. Initially, three boehmites were calcined at different temperatures to form different phases and tested for their decarboxylation performance. The reaction conditions such as temperature, amount of catalyst and amount of palladium on the support material were optimized for the best found aluminum oxide.

Subsequently, the best found aluminum oxide catalyst was mixed with different amounts of H–ZSM5 zeolite to improve the deoxygenation performance. Additionally, some selected process parameters, which previously showed a major influence on conversion rate and selectivity (dilution of hydrogen and weight hourly space velocity, WHSV) were optimized, too.

Based on those obtained results silica aluminates impregnated with Pd were investigated as catalysts for the deoxygenation

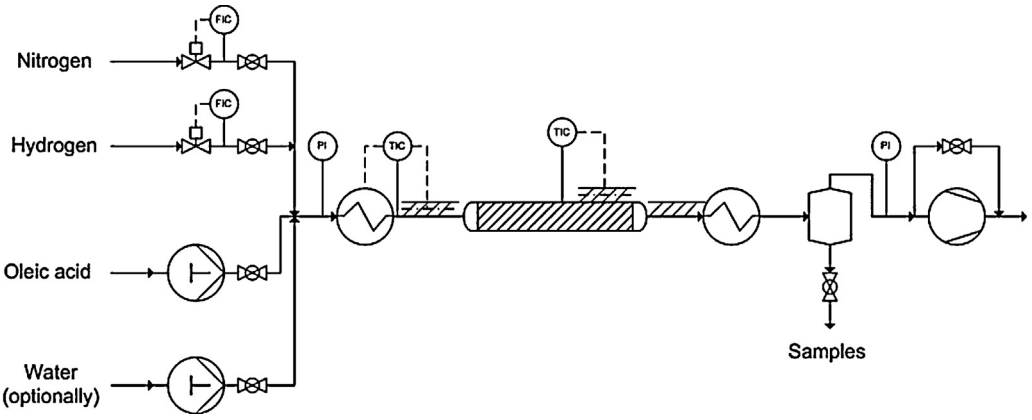

Fig. 1. Schematic plug-flow-reactor setup.

and cracking of free fatty acids. Special interest was paid to the composition of the product mixture and its sustainability for use as diesel-fuel.

2. Experimental

2.1. Chemicals and catalyst preparation

Oleic acid (Merck, extra pure, 65–88%), boron trifluoride in methanol (Fluka, ~10 wt.% BF_3) and methyl laurate (Fluka, purum) were used as received. Hydrogen (Praxair, 99.999%) and nitrogen (Westfalen, 99.999%) were purchased in ultra high purity. Palm oil and mixed fatty acid were kindly provided by ADM Research GmbH, Hamburg.

The pseudo-boehmites Pural SB1, Pural NG and Pural 200 as well as the amorphous silica aluminates (Siral 40, 70 and 80) were generously provided by Sasol as powders and extruded in-house. The zeolites used are obtained from Zeolyst International Conshohocken, PA, USA. The authors are very grateful to them for these donations.

For catalyst extrusion, about 100 g of pseudo-boehmite or Siral were mixed in a kneader with about 90 g of a 2 wt.-% aqueous acetic acid solution and kneaded for about 30 min to obtain a highly viscous clay-like material, which was extruded with a diameter of 1 mm. The catalyst was dried at 110 °C and afterwards calcined in a muffle furnace at temperatures between 500 °C and 1100 °C with a heating rate of 1 K/min for 6 h.

The palladium catalysts were prepared by wet impregnation method using hydrochloric $PdCl_2$ or an aqueous solution of tetraamine palladium nitrate solution in which palladium was dissolved as $[PdCl_4]^{2-}$ or $Pd(NH_3)_4(NO_3)_2$, respectively. Thereby, the support was mixed thoroughly with $PdCl_2$ solution and excess water was removed in a rotary evaporator. The impregnated catalyst was usually calcined at 550 °C for 6 h and thereafter reduced in a tube furnace under flowing hydrogen at 200 °C for 2 h.

Composite catalysts were extruded as described above. Thereby, a certain amount of boehmite or Siral powder was replaced by H–ZSM5 powder. 2 wt.% aqueous acetic acid solution were added to such mixtures which afterwards were kneaded, extruded, dried and calcined. Impregnation and reduction were accomplished as described above.

2.2. Catalyst characterization

The impregnated palladium content was determined by inductive coupled plasma method on a Spektro-Flame D. Sample preparation was carried out by storing the catalyst with concentrated HCl/HNO_3 for one week to assure complete dissolution of Pd. The clear solution was diluted with water and measured. Quantification was conducted via a comparison of the sample with certified calibration solutions.

The BET surface area was measured by means of nitrogen adsorption isotherms in the Micrometrics ASAP 2010 at 77 K and a partial pressure range p/p_0 of 0.05–0.25.

The spent catalysts were regenerated by calcination in air at 550 °C for 6 h before the BET surface areas were measured again.

Pyridine FT-IR spectroscopy was accomplished in a Nicolet Spektrometer type 460 Protege. The catalyst was grinded and mixed with KBr then pressed to form a tablet for the measurement. IR spectra were recorded at temperatures between 50 °C and 400 °C in a range of 1400–1800 cm^{-1}.

Ammonia temperature programmed desorption (TPD) analysis was conducted by means of Carlo Erba TPDRO 1100 Series Thermo Finnigan. Samples were degassed at 500 °C in helium and subsequently loaded with NH_3 at 30 °C. Desorption was performed in the range of 50–1000 °C using helium as carrier gas and a thermal conductivity detector.

Thermogravimetric analysis was done in a Netzsch STA 409 C by heating the sample from room temperature to 1100 °C with a ramp of 2 °C/min in dry air.

X-ray powder diffraction (XRD) patterns were measured on a Siemens D 5000 with Cu Kα1 (154.0598 pm) and Cu Kα2 (154.4426 pm wavelength). The scan was done in the 2θ range of 3–90° with 0.02° step width and 1s data acquisition.

Field emission scanning electron microscopy (FESEM) was carried out in a ZEISS DSM 982 Gemini of the "Gemeinschaftslabor für Elektronenmikroskopie (GFE)" at RWTH Aachen University.

2.3. Experimental setup

The catalytic tests for the continuous hydrodeoxygenation of oleic acid in the presence of all applied catalysts were carried out in a plug-flow-reactor system. It consisted of an evaporator and a reactor, both heated in air circulation ovens. Each oven was equipped with a thermocouple, and the temperature was controlled by a Eurotherm 902 with an accuracy of ± 1 °C. The evaporator was a stainless steel tube with an inner diameter of 6 mm, in form of a coil with an overall length of 160 cm. Furthermore, this tube was filled with glass beads (1.25 mm diameter) to ensure good evaporation by improving heat-transfer through surface enlargement.

The evaporator tube is directly connected to a stainless steel reactor in form of a coil (inner diameter 6 mm, overall length 80 cm). A wire mesh was located as catalyst chair at the end of the reactor in order to keep the catalyst in the reactor.

OA and water were pumped separately with two piston pumps (type: Latek P400). The hydrogen and nitrogen flows were

controlled via two mass-flow controllers (both: Brooks 5850E). The products were collected at the reactor outlet in a water chilled double jacket cooling trap. A schematic diagram of the setup is given in Fig. 1.

Typically, 3 g of granulated catalyst was placed in the reactor. Thereafter, the reactor was flushed thoroughly with N_2 to remove air. The H_2 flow was subsequently adjusted to the desired volumetric flow. Then the reactor was heated to the desired temperature. The reaction commenced as soon as the pump for the reactant was started. After the reaction, the reactor was cooled down to room temperature in nitrogen atmosphere and the catalyst was removed.

In addition the hydrodeoxygenation and cracking reactions in liquid phase were conducted in a trickle-bed-reactor. The trickle-bed-reactor consists of two gas inlets (hydrogen and nitrogen), each controlled by a mass flow controller of Brooks (V1 and V2). The mixed gases and liquids are preheated and passed into the reactor. The reactor consists of a vertical stainless steel tube with an inner diameter of 10 mm and a length of 75 cm. The pressure inside the reactor is controlled by a pressure release valve. The reactants and the solvents used for cleaning purposes can separately be pumped into the reactor (C1) with two high pressure piston pumps (P1 and P2) type Latek-P400. The products are collected in a water chilled double-jacked cooling trap. A schematic flow chart of the setup is given in Fig. 2.

2.4. Product analysis

The collected samples were esterified with methanol to increase the volatility of the free fatty acids before its quantification by means of GC analysis. This was carried out by mixing the sample with 100 wt.-% excess of BF_3 in methanol. After heating at 60 °C for 30 min, the organic products were extracted with approximately 5 fold excess in weight of pentyl myristate, washed with water and dried over sodium sulfate. The internal standard methyl laurate was subsequently added for quantitative calculations. The samples were analyzed by the means of the gas chromatograph Siemens RGC202, equipped with a flame ionization detector (FID) and a FS-CW-20M (50 m) column. (Deletet) 2 μl of the sample were injected with a constant carrier gas pressure (Helium, Westfalen, 99.999%) of 1.5 bar. The used temperature program was: 50 °C for 2 min, 240 °C (ramp 10 °C/min) held for 30 min. Injector and detector temperature were 280 °C, respectively. The peaks were integrated using a Spectra Physics no. 4270 device. The GC accuracy was verified in several experiments, giving constant results with an overall error of the analysis below 0.5%.

The composition of the reactant oleic acid needs to be considered for quantification purposes. It contained 85.6 mol% oleic acid, 6.0 mol% linoleic acid, 2.9 mol% stearic acid and 5.5 mol% palmitic acid. For calculating the conversion X, the total amount of the C18 acids (stearic-, oleic- and linoleic acid) was combined and considered as one component.

$$X = \sum_i \frac{n_i}{n_{\mathrm{C18Acids,in}} - n_{\mathrm{C18Acids,out}}}$$

The calculation of selectivities for the decarboxylated products was carried out individually for every single component i and combined in the end into the total C17 selectivity (S)

$$S = \sum_i \frac{n_i}{n_{\mathrm{C18Acids,in}} - n_{\mathrm{C18Acids,out}}}$$

3. Results and discussion

3.1. Reaction scheme

The suggested deoxygenation reactions of oleic acid are displayed in Fig. 3.

In a first reaction step, oleic acid (1) is either hydrogenated, forming stearic acid (2) or is decarboxylated to *n*-8-heptadecene (3) and its isomers. Subsequently, SA has to be decarboxylated and

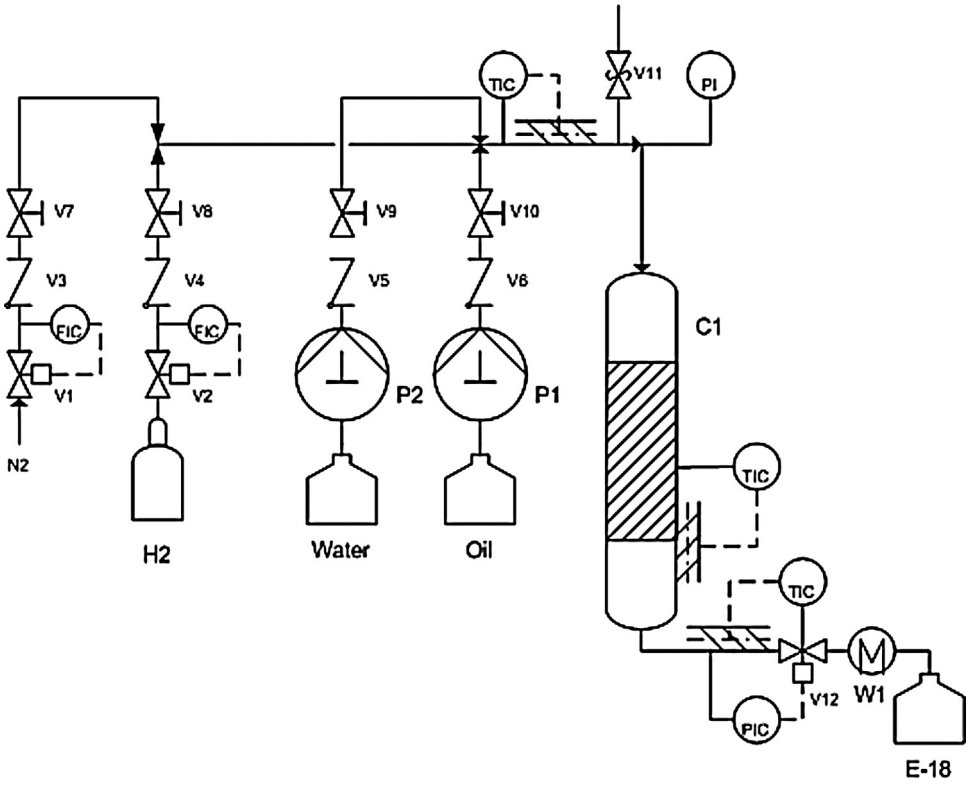

Fig. 2. Schematic trickle-bed-reactor setup.

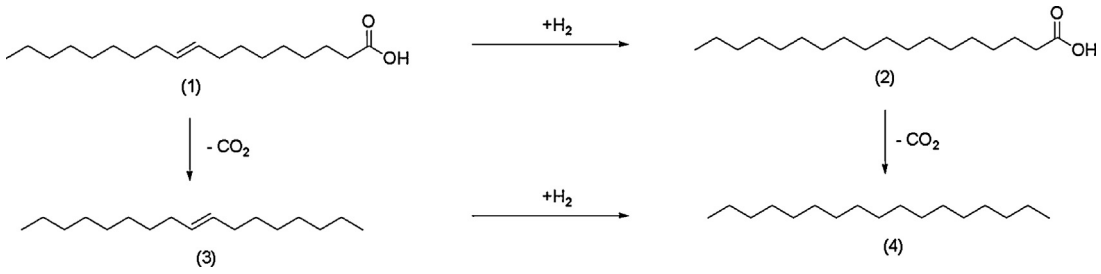

Fig. 3. Reaction scheme: deoxygenation of oleic acid.

the heptadecenes have to be hydrogenated, respectively, in order to form the saturated *n*-heptadecane (4).

Additionally, oleic acid can also be decarbonylated in inert atmospheres, which forms the di-unsaturated heptadecenes (all isomers), as proposed by Şenol et al. [21]. Possible side reactions are cracking reactions to shorter chain hydrocarbons, hydroisomerization, polymerization and aromatization.

3.2. Aluminum oxide catalysts

3.2.1. Characterization of pure aluminum oxide supports

Different aluminum oxide phases are obtained by the various calcination conditions as identified by XRD. The XRD patterns of Pural SB1 as example (Fig. 4) show generally highly amorphous aluminum oxides with exception of the crystalline α-phase. For calcination temperatures up to 700 °C only the γ- phase was observed, whereas for 800 °C and 900 °C mixed γ- and δ- phase were found, with an increasing amount of the δ- phase for higher calcination temperatures. At 1000 °C calcination temperature mixed δ- and θ-phase and for 1100 °C the crystalline α- phase (corundum) were detected.

Generally, all pseudo-boehmites we applied as support were calcined at temperatures between 550 °C and 1100 °C (Pural SB1 was additionally calcined at 500 °C) where the formed aluminum oxide phases were found as described before.

The BET surface area of Pural SB1 calcined at 550 °C was 216 m^2/g and BJH average pore radius 34.4 Å. Pural NG had a BET surface area of 154 m^2/g and BJH average pore radius 49.0 Å. In contrast, Pural 200 showed only 72 m^2/g BET surface area but a BJH average pore radius 142.5 Å.

Ammonia TPD measurements of the γ-aluminium oxides (all materials calcined at 550 °C) clearly illustrated that the one based on the Pural SB1 precursor resulted in the most acidic catalyst followed by Pural NG and Pural 200 as illustrated in Fig. 4.

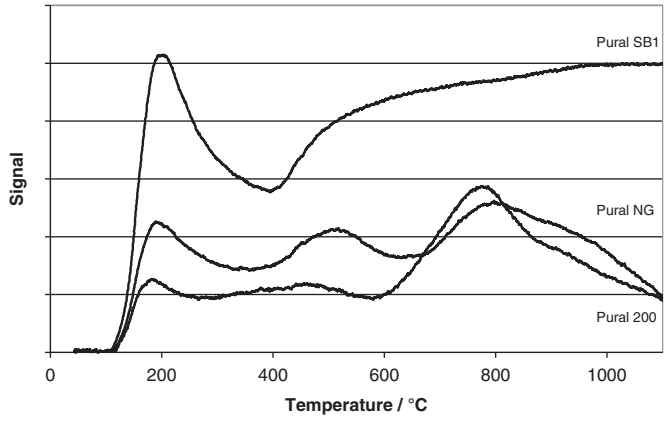

Fig. 4. Ammonia TPD of Pural SB1, Pural NG and Pural 200.

The signals at 200 °C indicate weak acidic sites, whereas the peaks at 500 °C were caused by strong acidic sites. The approaching peak at 800 °C is probably due to further phase transitions.

As example pyridine FT-IR of Pural SB1 calcined at 550 °C indicated predominantly Lewis acidic sites. The spectrum was taken at 100 °C which and showed predominantly Lewis acidic sites (5). The signal at 1457 cm^{-1} clearly indicated the Lewis-acidity of the catalyst. A minor Brønsted acidity was observed at 1620 cm^{-1}.

All the other materials show the same features.

3.2.2. Screening of the aluminum oxide based catalysts

All aluminum oxides were impregnated with 1 wt.% Palladium using $Pd(NH_3)_4(NO_3)_2$ solution and subsequently tested in the plug flow unit (Fig. 1) at 380 °C reaction temperature, hydrogen flow of 50 ml/min, 3 g of catalyst and an OA flow of 5.6 g/h, which resulted in a WHSV of 1.9 h^{-1}. The results obtained after 4 h time on stream are summarized in Table 1.

Two C17-selectivity maxima were observed for all Pural precurors. The first maximum was found at a calcination temperature of 550 °C and the second was found at 900 °C. These are the γ-aluminum oxide phase or the mixed γ- and δ- phase. However, the γ- phase was catalytically most active and gave the best C17 selectivities. The Pural SB1 based catalyst yielded the best selectivity for C17-products among all tested catalysts based on the other Pural precursors. Pural SB1 was also calcined at 500 °C to investigate its catalytic performance. In this case the selectivity to the desired C17 products was lower compared to the aluminum oxide Pural SB1 calcined at 550 °C at almost the same conversion. Catalyst stability was not tested.

The conversion rate obtained with Pural SB1 and Pural NG were in a range of 78–97 mol%, except for the crystalline α- phase in which conversion only reached about 29 mol% and 22 mol%, respectively. The use of Pural 200 as support resulted in significantly lower conversions of about 59–81 mol% for all experiments, but surprisingly a higher rate of 45 mol% was achieved for the α- phase based catalyst. This was possibly due to the different physical properties of the precursors such as surface areas and different number of acidic sites (see Fig. 5). The most acidic catalyst originated from Pural SB1 with the largest BET surface area and highest number of acidic sites resulted in the best catalytic performance.

The formation of gaseous products was in the range of 6– 17 wt.-% of the amount of reactant pumped into the reactor. A complete decarboxylation of oleic acid would result in a mass loss of 14.8 wt.-% by CO_2 elimination. As the highest obtained decarboxylation rate based on the found products was about 51 wt.-%, the mass loss by CO_2 formation could be consequently at most 7.5 wt.-%. The gas analysis showed the existence of CO_2 and minor amounts of CO, methane and propane, which explains further mass loss by liquid products. Exact gas phase compositions could not be determined due to technical limitations. In addition coke formation, polymerization and liquid residues in the reactor setup are also possible explanations for such findings and cannot be completely excluded.

Table 1
Screening of the catalysts based on different Pural precursors.

Precursor pural	Calcination temperature	Conversion	Gaseous products[a]	Selectivity	
				stearic acid	C17 products[b]
	°C	mol%	wt%	mol%	
SB-1	500	89.1	15.8	8.5	38.1
	550	87.2	12.9	10.1	50.7
	600	89.8	13.2	9.0	45.4
	700	97.3	15.5	6.0	41.4
	800	90.5	14.3	7.1	35.1
	900	95.3	15.2	8.2	41.7
	1000	78.0	10.0	10.0	35.4
	1100	29.0	5.6	8.0	2.6
NG	550	86.2	13.4	9.5	37.4
	600	93.8	12.0	7.9	29.0
	700	94.1	12.1	7.5	25.5
	800	85.1	12.7	16.8	32.0
	900	82.8	9.4	11.1	35.5
	1000	88.3	15.1	8.3	33.9
	1100	22.2	4.2	5.5	4.4
200	550	81.5	11.7	8.1	36.3
	600	76.0	9.5	6.2	30.3
	700	73.6	10.5	6.6	28.9
	800	69.1	11.1	7.0	19.1
	900	68.2	9.9	8.0	25.2
	1000	59.3	13.6	9.4	23.0
	1100	45.3	6.8	8.6	9.8

[a] Calculated as difference of mass pumped in the reactor and all collected liquids.
[b] Summed up selectivity of all C17 products: *n*-heptadecane and all heptadecene isomers.

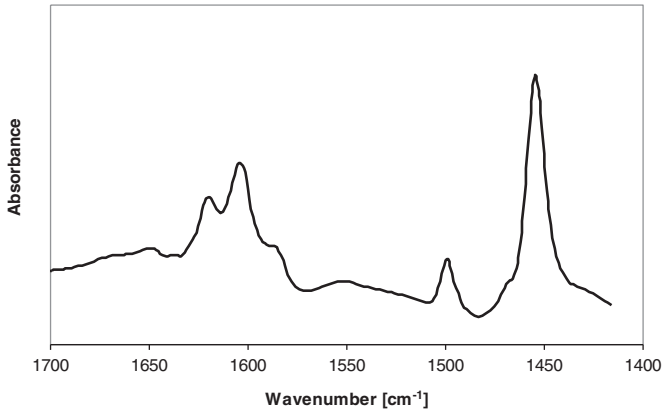

Fig. 5. Pyridine FT-IR of Pural SB1.

3.2.3. *Influence of process parameters*

Catalysts based on aluminum oxides calcined at 550 °C and doped with 1 wt.-% palladium were found as to be the best in the screening. The catalyst based on Pural SB1 which was superior over the others was consequently used for studying the influence of different process parameters on the conversion and selectivity after 4 h time on stream.

The influence of the reaction temperature is elucidated in Table 2.

The minimum reaction temperature was kept 20 °C above the boiling point of OA at atmospheric pressure (360 °C) to ensure a complete gas phase reaction. Increasing conversion but the simultaneous decrease of the C17 selectivity at higher reaction temperatures was observed. The selectivity drop is due to increased thermal and catalytic cracking and decomposition generating more gaseous products.

Table 3
Different amount of catalyst.

Amount of catalyst	1 g (WHSV = 5.6/h)	3 g (WHSV = 1.9/h)	5 g (WHSV = 1.1/h)
Conversion	61.3	89.0	99.3
C17 selectivity	24.6	47.2	33.8

The amount of catalyst employed in the reaction was varied from 1 g to 5 g as presented in Table 3.

The amount of catalyst corresponds to the weight hourly space velocity (WHSV) which was varied from 5.6 h^{-1} for 1 g to 1.1 h^{-1} for 5 g. For high WHSV and accordingly low catalyst amount, conversion and selectivity were lower compared to higher catalyst amounts. For 3 g of catalyst, the best C17 selectivity was obtained. For the highest applied catalyst amount, an increased formation of gaseous products was observed due to consecutive stronger cracking processes.

To determine the influence of palladium content on the catalyst performance, experiments with pure aluminum oxide as well as catalysts with varying palladium amounts were accomplished. The results are illustrated in Table 4.

The catalyst based on γ-aluminum oxide Pural SB1 calcined at 550 °C without palladium led to a conversion of 50 mol%, but no desired C17 products were observed. However that support doped with 0.5 wt.-% palladium yielded a conversion of 90 mol.-%. The

Table 2
Influence of the reaction temperature.

Reaction temperature	380 °C	415 °C	450 °C
Conversion	89.0	92.6	97.7
C17 selectivity	47.2	14.6	1.7

Table 4
Different amount of palladium.

Amount of palladium	0% Pd	0.5 % Pd	1% Pd	2% Pd
Conversion	50.0	90.5	89.0	99.1
Selectivity C17	0.0	29.8	47.2	46.7

conversion was increased to 99 mol% for the material doped with 2 wt.-% Pd. The selectivity of the C17 products was 30 mol% for the lowest Pd amount but was increased to 51 mol% for 1 wt.-% Pd and to 47 mol% for 2 wt.-% Pd, respectively. As the higher Pd amount did not result in a further improvement of the selectivity it can be stated that the maximum decarboxylation activity was achieved already over a catalyst with 1 wt.-% Pd.

3.3. Mixed aluminum oxide/H–ZSM5 catalysts

3.3.1. Catalyst characterization

Based on the above mentioned results, aluminum oxide was mixed with different amounts of H–ZSM5 in order to increase the acidity of the catalyst and consequently the cracking and decarboxylation performance. Catalysts (C) are labeled according to their aluminum oxide content (CAl_{20} corresponds to 20 wt.-% aluminum oxide; CAl_{100} corresponds to 100 wt.% aluminum oxide). The XRD patterns of the pure aluminum oxide CAl_{100} indicate highly amorphous material. 5 wt.-% H–ZSM5 in aluminum oxide already showed a characteristic zeolite peak in the XRD patterns. This peak steadily increased with higher content of zeolite in the composite.

Acidity of the applied catalysts was determined by ammonia TPD measurements. Increasing acidity was observed for higher zeolite ratios in the composite. Weak acidic sites were observed at 200 °C and strong acidic sites were obtained at 450 °C/500 °C. The minor signals above 750 °C were probably caused by further phase transformation of the aluminum oxide.

The BET surface area of the pure Pural SB1 derived γ-aluminum oxide (calcined at 550 °C) was 216 m^2/g and BJH average pore radius 34.4 Å. In comparison, the surface area of CAl_{80} was 223 m^2/g and BJH average pore radius 48.3 Å. Higher ratios of zeolite in the composites resulted in larger BET surface areas and BJH average pore radius.

Catalyst CAl_{80} was regenerated 5 times by thermal treatment at 550 °C for 6 h in air. The BET surface area after these treatments dropped slightly to 215 m^2/g and the BJH average pore radius was 53.7 Å. Thus, it can be concluded that the surface area was not significantly influenced by regeneration.

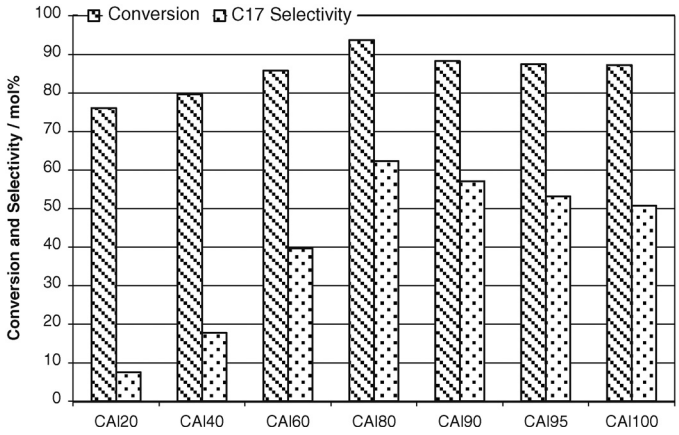

Fig. 6. Catalyst screening for different mixtures of aluminum oxide/H–ZSM5; reaction conditions: T = 380 °C; $\dot{V}_{H_2}$ = 50ml/mn; $\dot{m}_{OA}$ = 5.6g/h, $m_{Catalyst}$ = 3 g, all catalysts were impregnated with 1 wt.% Pd.

3.3.2. Catalyst screening of the aluminum oxide/HZSM-5 composites

All catalysts were impregnated with 1 wt.% palladium using $Pd(NH_3)_4(NO_3)_2$ solution and subsequently tested in the plug flow rector at 380 °C, a hydrogen flow of 50 ml/min, 3 g of catalyst and an OA flow of 5.6 g/h, which results in a WHSV of 1.9 h^{-1}. Fig. 6 shows the obtained conversion and C17 selectivity for the used catalyst mixtures.

The conversions presented in Fig. 6 is the average over 6 h TOS (= time on stream). The conversion increased hereby from 76 wt.-% for the lowest aluminum oxide amount (CAl_{20}) to a steady state level of about 90 wt.-% for catalysts with aluminum oxide contents higher than 80 wt.-% (CAl_{80}). The overall best C17 selectivity of 62 mol% was found for the mixture of 80 wt.-% aluminum oxide and 20 wt.-% H–ZSM5 at a conversion of 94%. For higher aluminum oxide contents the C17 selectivity dropped to the aforementioned 51 mol% for pure aluminum oxide catalysts. Catalysts which contained higher amounts of zeolite resulted in high cracking activity in the first hour TOS, but then it decreased with longer TOS. Catalysts without zeolite did not show this behavior of initially high cracking activity. Additionally, only in the first two hours TOS a minor selectivity for aromatic products of about 10 mol% was found for

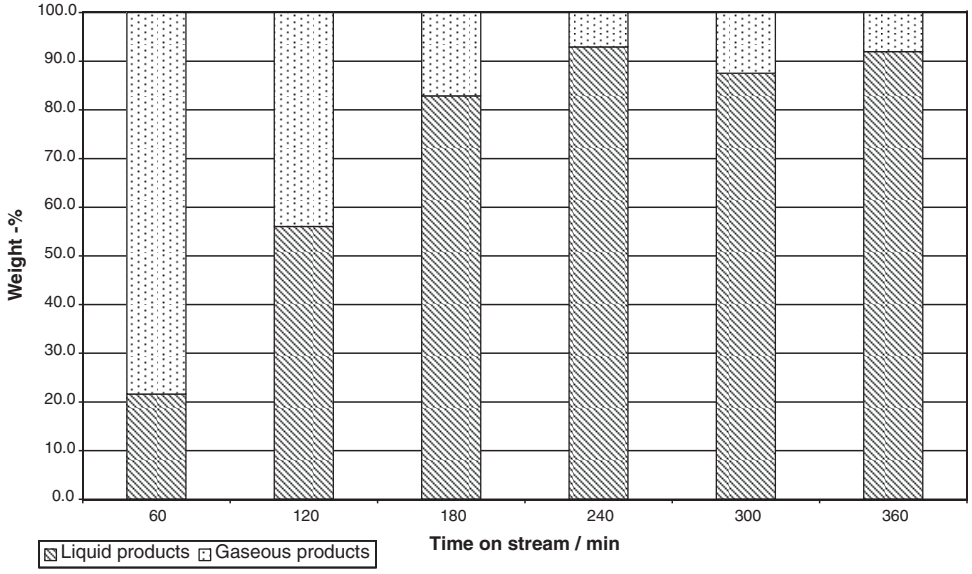

Fig. 7. Liquid and gaseous products obtained over CAl_{80} impregnated with 1 wt.% Pd; reaction conditions: T = 380 °C; $\dot{V}_{H_2}$ = 50ml/mn; $\dot{m}_{OA}$ = 5.6g/h, $m_{Catalyst}$ = 3 g.

Table 5
Catalysts based on amorphous silica aluminates as supports.

Name	Siral [wt.-%] (module)	Zeolites [wt.-%] (module)	Pural SB-1 [wt.-%]	Pd precursor
1 wt.-% Pd/Siral40	Siral (40) [90]	/	10	$PdCl_2$ sol.
1 wt.-% Pd/Siral70	Siral (70) [90]	/	10	$PdCl_2$ sol.
1 wt.-% Pd/Siral70/20H–ZSM5_50	Siral (70) [70]	H–ZSM5 (50) [20]	10	$Pd(NH_3)_4(NO_3)_2$ sol.
1 wt.-% Pd/Siral70/10H–ZSM5_1000	Siral (70) [80]	H–ZSM5 (1000) [10]	10	$Pd(NH_3)_4(NO_3)_2$ sol.
1 wt.-% Pd/Siral80	Siral (80) [90]	/	10	$Pd(NH_3)_4(NO_3)_2$ sol.

The module of the sirals equals to the silica amount of the sirals in wt.-% and the module of the zeolites is the ratio of SiO_2/AlO_2.

zeolite containing catalysts. The lower overall conversion for high zeolite containing composites was due to deactivation of the very strong acid sites of the catalyst during the first hours of TOS, caused by deposits of coke on the catalyst surface blocking the active sites.

Thermogravimetric analysis of the spent catalyst showed a mass loss of about 25 wt.-% which was caused by carbonaceous residues on the catalyst surface. Fig. 7 shows the mass balance which was calculated as the difference of the liquid pumped into the reactor and the collected liquid in the cooling trap.

In the beginning of the reaction gaseous products such as CO_2, CO, CH_4 and propane were formed due to the high cracking activity by the very strong acid sites of the zeolite. With longer TOS some acidic sites were deactivated by carbonaceous materials like coke, polymers and high boiling liquid residues. Because of this deactivation, the formation of gaseous products dropped to a constant level of about 10 mol% after 3 h TOS.

3.4. Silica aluminates and mixed silica aluminates/zeolite based catalysts

In Part 3.2 and 3.3, the main products are *n*-heptadecane and heptadecenes with total selectivities of 62% at 94% conversion. Because of their high boiling point these C17- products can only be used as a blend in regular diesel. Therefore, amorphous silica–alumina based catalysts having higher acidity and therefore higher cracking activity were tested with the intention to obtain diesel like product mixtures consisting of generally saturated hydrocarbons with C-6–C-18 chain length. Amorphous silica–aluminates with different Si/Al ratios and accordingly with different strengths of Brønsted acidity were investigated. It was observed, that in contrast to the former investigations over alumina–zeolite based catalysts the C-17 selectivity decreased and a wide range of short-chain hydrocarbons were found.

3.4.1. Catalyst characterization

All catalysts were impregnated using $Pd(NH_3)_4(NO_3)_2$ or $PdCl_2$ solution. The XRD patterns of all these catalysts were measured, but no specific crystal structure could be determined as the crystal domains of Pd were too small. Moreover, all XRD patterns of the characterized catalysts show an amorphous band between 20° and 40°.

Inductive coupled plasma method (ICP) was carried out to quantify the Pd amount of the catalysts. Quantification was conducted via a comparison of the sample with certified calibration solutions.

The BET surface area of the 1 wt.-% Pd/Siral 40 catalyst was 350 m^2/g and BJH average pore radius was 38.5 Å. In comparison, the surface area of 1 wt.-% Pd/Siral 70 catalyst was 328 m^2/g and the BJH average pore radius 38.3 Å. In the case of 1 wt.-% Pd/Siral 80 catalyst 304 m^2/g and a BJH average pore radius of 54.7 Å were found i.e., the smallest surface area but the largest pore radius. Higher silica ratios in the amorphous silica aluminate supports resulted in smaller BET surface areas and BJH average pore radius.

3.4.2. Continuous gas phase reactions

The catalysts applied in the plug flow reactor are given in Table 5.

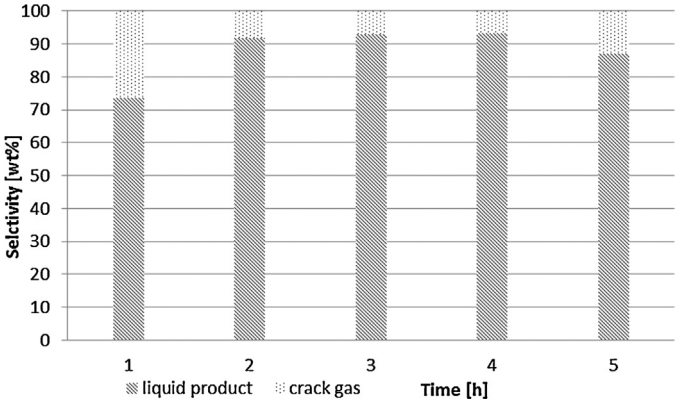

Fig. 8. Yields of crack gas and liquid products with 1 wt.-% Pd/Siral70, reaction conditions: $T = 380\,°C$; $\dot{V}_{H_2} = 104.4\,ml/min$; $\dot{m}_{OA} = 5.1\,g/h$, $m_{Catalyst} = 3\,g$.

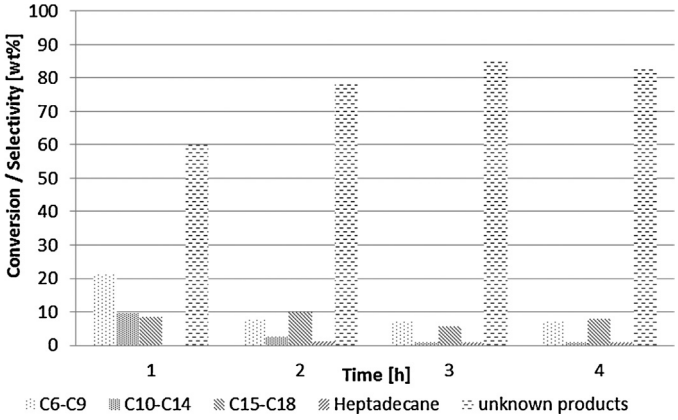

Fig. 9. Liquid product distribution over 1 wt.-% Pd/Siral70, reaction conditions: $T = 380\,°C$; $\dot{V}_{H_2} = 104.4\,ml/min$; $\dot{m}_{OA} = 5.1\,g/h$, $m_{Catalyst} = 3\,g$.

10 wt.-% Pural SB1 was added to each catalyst in order to achieve the needed mechanical strength of catalyst particles to withstand reaction conditions without breaking apart.

For the gas phase experiments we used 3 g of catalyst, a reaction temperature of 380 °C and ambient pressure. The incoming feed was 5.1 g/h oleic acid and 104.4 ml/min hydrogen which results in a WHSV of 1.85 h^{-1}. In all these gas phase experiments a constant conversion of oleic acid of 100 wt.% is observed.

The best result, according to a wide product distribution of C-7–C18 hydrocarbons was achieved with the 1 wt.-% Pd/Siral70 catalyst. As demonstrated in Fig. 8, the selectivity to liquid products increases under simultaneous decrease of crack gases over reaction time.

The distribution of the liquid products is illustrated in Fig. 9. The selectivity to the desired hydrocarbons with C-7–C-18 chain length decreases and the formation of unidentified compounds with a boiling point below the boiling point of oleic acid (≈330 °C) increases.

The unidentified products seem to be C17 and C18 hydrocarbons which are most likely branched. Due to their boiling point below 330 °C they can be used as a good diesel blend.

The change of the liquid product distribution can be explained by deactivation of the catalysts due to coke formation blocking the catalytically active centers and causing decreased surface area.

In the case of the 1 wt.-% Pd/Siral40 and 1 wt.- % Pd/Siral80 catalysts, similar results were obtained but the product selectivity was a bit lower. The mixed silica-alumina/zeolite catalysts 1 wt.-% Pd/Siral70/10H–ZSM5_1000 and 1 wt.-% Pd/Siral70/20H–ZSM5_50 have strong cracking activity whereby the selectivity to gases products were increased but the selectivity of the liquid products was much lower.

According to our former investigations the reaction temperature of 380 °C was found to be the optimum. In addition the residence time influence had to be studied. The mass of catalyst in the reactor was varied from 3 g to 4 g up to 5 g i.e., a decreasing WHSV and an increased residence time. The best yield for the liquid products was obtained using 3 g of catalyst whereas the selectivities to the liquid products were similar in all experiments. Therefore, the use of only 3 g of catalyst (Fig. 8) was found to be suitable and more economical.

Steam was added to the reactant feed in mass ratio of 1, in order to facilitate the desorption of the reaction products, to suppress coke formation and eventually to improve the conversion, selectivity and catalyst life time. The coke formation was reduced by the addition of steam but simultaneously a decrease of the liquid product yield was observed. The selectivity to stearic acid increases by the addition of steam.

3.4.3. Continuous liquid phase reactions in trickle bed reactor

3.4.3.1. Reactions at ambient reaction pressure (H_2). The cracking reaction was conducted in the liquid phase to obtain better selectivities of C-7–C18 hydrocarbons. Therefore, the reaction setup was modified from a continuous plug-flow-reactor into a continuous trickle-bed-reactor. Different silica alumina based catalysts were tested (Table 6). Also mixed silica alumina–zeolite catalysts were tested but their activity to the desired products were lower.

The process parameters like temperature, reactant feed and WHSV were varied. The best results were obtained by using 15 g of catalyst (1 wt.-% Pd/Siral70), at a reaction temperature of 350 °C and a reactant flow of 18.3 g/h (WHSV: 1.85 s^{-1}). In all liquid phase experiments a conversion of oleic acid of 100 wt.% is observed.

The other tested catalysts based on pure silica–alumina supports (1 wt.-% Pd/Siral40 and 1 wt.-% Pd/Siral80) resulted in very similar catalytic performance and product distribution.

The yield of crack gases decreased with longer TOS and the yield of liquid product increased (Fig. 10). This observation can be explained by the deactivation of the strongest active catalytic sites after two hours TOS. That trend was found for all applied catalysts.

When the yield of liquid products increases, the product selectivity decreases and higher boiling unidentified components (boiling point below 300 °C) are formed as illustrated in Fig. 11. The higher boiling compounds have a similar distillation behavior shown in Fig. 14).

Using the same catalyst, the selectivities for C-6–C18 hydrocarbons is higher in the liquid phase reaction after one hour TOS than compared with the gas phase reaction. The product selectivities approach a steady state after two hours TOS and maintain on the same level until the reaction ends.

Table 6
Catalysts tested in the continuous liquid phase reaction of oleic acid.

Name	Siral [%] (module)	Pural SB-1 [%]
1 wt.-% Pd/Siral40	Siral (40) [90]	10
1 wt.- % Pd/Siral70	Siral (70) [90]	10
1 wt.- % Pd/Siral80	Siral (80) [90]	10

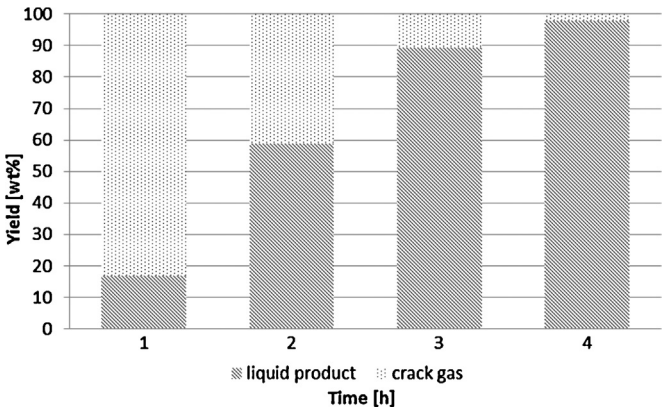

Fig. 10. Yields of crack gases and liquid products with 1 wt.- % Pd/Siral70, reaction conditions: T = 350 °C; $\dot{V}_{H_2}$ = 237.3ml/min; $\dot{m}_{OA}$ = 18.3g/h, $m_{Catalyst}$ = 15 g.

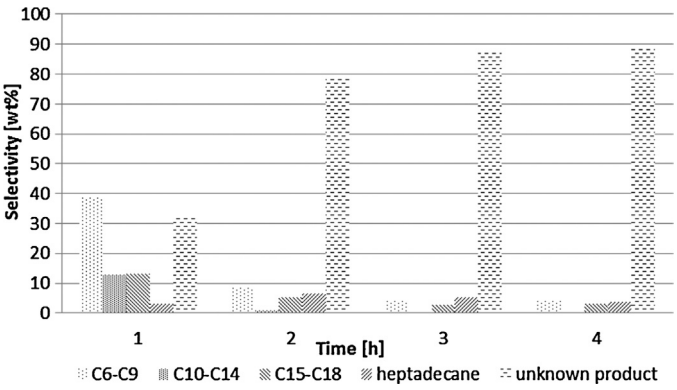

Fig. 11. Liquid product distribution with 1 wt.-% Pd/Siral70, reaction conditions: T = 350 °C; $\dot{V}_{H_2}$ = 237.3ml/min; $\dot{m}_{OA}$ = 18.3g/h, $m_{Catalyst}$ = 15 g.

Fig. 12 illustrates the gas chromatogram of a sample obtained in an experiment using 1 wt.-% Pd/Siral70 after one hour time on stream in comparison with the GC of a sample of conventional diesel of a refinery. The product distribution of that sample is very similar to conventional diesel. Thus, the product mixture obtained after one hour TOS could be used directly as an alternative green fuel and not only as a blend of conventional diesel.

All experiments in the presence of these Siral/zeolite mixed catalysts result in a lower yield of liquid products and a lower selectivity to the desired C-6–C18 hydrocarbons than over the catalysts based on pure silica–alumina catalysts. The lower yield of liquid products can be explained with the very high acidity of the zeolites resulting in more gas formation, i.e., short chained hydrocarbons (C-1–C-4). The lower selectivity to C-6–C-18 hydrocarbons were due to the high cracking activity.

3.4.3.2. Reactions under elevated reaction pressure (H_2). Three different reaction pressures 5 bar, 10 bar and 15 bar were adjusted. The higher the pressure the higher the residence time of the reactants in the reactor at the beginning of the reaction and therefore the cracking reactions were slightly increased. Related to that, more gaseous products were obtained in the beginning of the experiment. After four hours TOS, the yields are nearly constant. The reaction under 5 bar pressure resulted in better product selectivities than the reaction under atmospheric pressure. Especially, the selectivity to heptadecane and unknown products decreased. By raising the pressure to 10 and 15 bar, the trend to higher diesel like

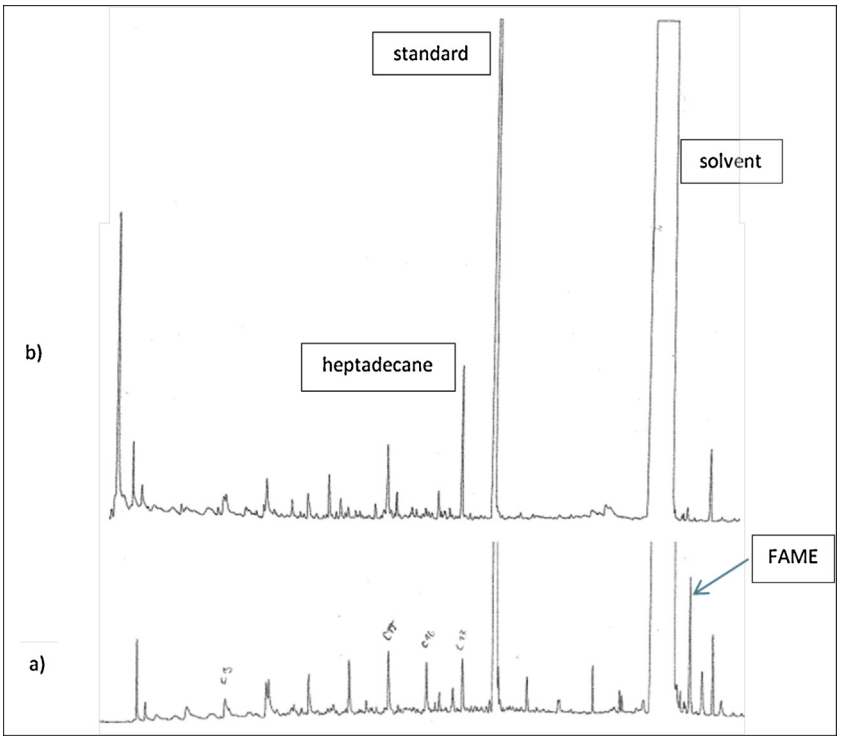

Fig. 12. Gas chromatograms of (a) conventional diesel and (b) experiment with 1 wt-% Pd/Siral70, reaction conditions: T = 350 °C; $\dot{V}_{H_2}$ = 237.3ml/min; $\dot{m}_{OA}$ = 18.3g/h, $m_{Catalyst}$ = 15 g.

product selectivities can be verified. Fig. 13 demonstrates the liquid product distributions for the reaction under 15 bar pressure.

After two hours TOS, the yields of liquid products range between 80 and 90 wt.% until the end of the reaction and the product selectivity for C6–C18 hydrocarbons in the liquid products maintains constant around 75 wt.-%.

The results obtained over the Siral/zeolites mixed catalysts under elevated reaction pressure were not as good as over the pure silica–aluminates based catalysts, 1 wt.-% Pd/Siral70, 1 wt.-% Pd/Siral40 and 1 wt.-% Pd/Siral80. As before, the best results were obtained in the presence of the 1 wt.% Pd/Siral70 catalyst.

The catalytic performance of 1 wt.-% Pd/Siral70 under the conditions, $m_{Cat.}$: 15 g, T: 350 °C, reactant feed: 18.3 g/h OA: 237.3 mL/min H_2, 15 bar yields the best product selectivity of all experiments and therefore a distillation according to DIN 51 751 was carried out.

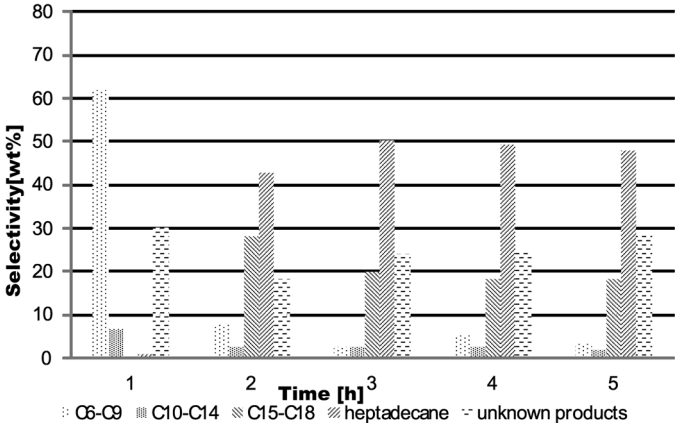

Fig. 13. Liquid product distribution with 1 wt.-% Pd/Siral70, reaction conditions: T = 350 °C; $\dot{V}_{H_2}$ = 237.3ml/min; $\dot{m}_{OA}$ = 18.3g/h, OA; 237.3 mL/min H_2, 15 bar.

The distillation of 100 mL product (all product after 10 h TOS) was compared to the distillation of 100 mL conventional diesel (Fig. 14).

The start- and end-points of the distillations were equal and the saddle point in the distillation shows a high selectivity for heptadecane. The distillation according to DIN 51 751 demonstrates that the product mixture with the corresponding product distribution can be excellent blended with conventional fuels also in very high amounts or maybe even used directly as diesel. Based on these findings it was concluded that the unidentified unknown products (Fig. 13) with a boiling point between 290 °C and 305 °C have very similar properties to conventional diesel.

3.4.4. Use of a mixture of fatty acids and palm oil

A mixture of fatty acids and crude palm oil – kindly provided by ADM – are non-eatable waste products out of the production of eatable oils. The palm oil is solid at room temperature because it contains triglycerides as well.

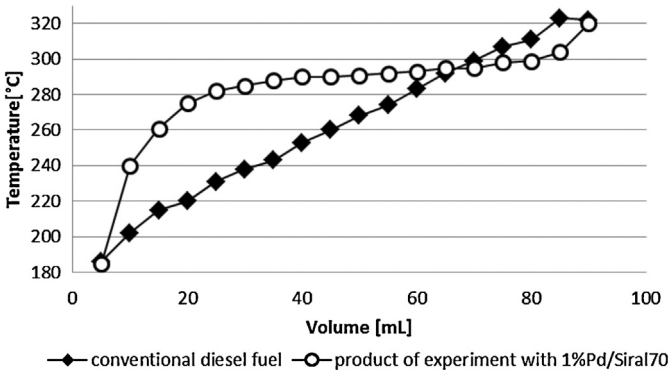

Fig. 14. Distillation according to DIN 51-751 of conventional diesel fuel and a product mixture obtained with 1 wt.-% Pd/Siral70.

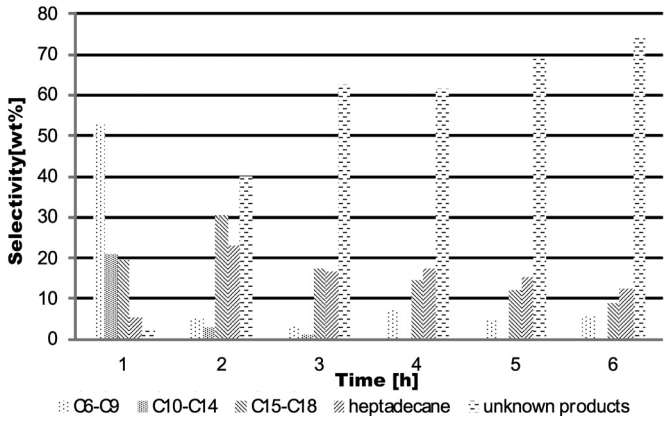

Fig. 15. Liquid product distribution using a mixture of free fatty acids and palm oil, 1% Pd/Siral70, reaction conditions: T= 350 °C; $\dot{V}_{H_2}$ = 237.3ml/min; $\dot{m}_{\text{re ac tant}}$ = 18.3g/h, m_{Catalyst} = 15 g, 15 bar.

A mixture of free fatty acids which contains other fatty acids in addition to our model compound oleic acid was used in a gas phase reaction (plug flow reactor (Fig. 1)). The observed product distributions are very similar to that found with oleic acid. (see Fig. 9). These results prove that not only the use pure oleic acid, but also other fatty acids react in the presence of the 1 wt.-% Pd/Siral70 catalysts to a diesel like fuel or to an excellent fuel blend. The presence of other fatty acids does not affect the main reactions.

Afterwards, the same free fatty acid mixture was tested as reactant in the liquid phase reaction (trickle bed reactor (Fig. 2)). Also in the trickle bed reactor the conversion of a mixture of free fatty acids results in a product distribution which is similar as in the case of pure oleic acid. The selectivities of C6–C18 hydrocarbons obtained over 1 wt.-% Pd/Siral70 catalysts 15 bar hydrogen pressure is lower and can be explained with contaminants in the mixture, which can be easier converted to coke. This coke formation lowers the catalytic activity.

Also a mixture of free fatty acids (80 wt.-%) and palm oil (20 wt.-%) were tested as feed in the liquid phase reaction using the 1 wt.-% Pd/Siral70 catalyst. (Fig. 15) shows that the product distribution and the selectivity is a little lower compared with the use of pure oleic acid as feed. Possible contaminations in the provided mixture may block the micropores and active centers of the catalyst. Thereby, the catalyst loose activity and selectivity to the desired products.

4. Conclusion

A maximum selectivity toward C17- products *n* heptadecane and all heptadecene isomers) of 51 mol% at a conversion rate of 87 mol% was found for a Pd-catalyst based on Pural SB1 derived aluminum oxide support which were calcined at 550 °C forming thereby the highly active γ-phase. Among the tested boehmite precursors, Pural SB1 derived aluminum oxide was the most acidic catalyst performing the highest conversion and C17 selectivity. Low reaction temperatures of 380 °C and moderate weight hourly space velocities of 1.9 h^{-1} were most suitable for highest C17 selectivity. The optimum amount of palladium on the catalyst was found to be 1 wt.-%.

A mixture of 80 wt.-% aluminum oxide and 20 wt.-% H–ZSM5 as precursor for the Pd- catalyst resulted in a C17 selectivity of 62 mol% at a conversion rate of 94 mol%. This catalyst was more acidic than the catalyst based on pure aluminum oxide, but less acidic than pure zeolite catalyst which showed high cracking activity to form gaseous products. It was therefore anticipated that enhanced catalytic performance be probably achieved over catalysts with medium acid strength.

Additionally, the pure aluminum oxide had an average pore diameter of 34.4 Å, whereas the average pore diameter was 48.3 Å for the 20 wt.-% zeolite containing catalyst. The larger pore size of the zeolite containing catalyst provided less diffusion hindrances for the large oleic acid molecules enhancing the catalytic performance.

Also catalysts based on silica–aluminates (Siral Si/Al mixtures) and Siral–zeolite mixtures, impregnated with 1 wt.-% Pd were applied. The conversion of oleic acid was about 100% in all experiments during the test. The yield of all liquid products increased with TOS but the product selectivity for the C-6–C-18 compounds decreased. That means the cracking ability of the catalysts decreases.

With respect to C6–C18 hydrocarbons, the best results (40% yields of diesel fraction) in gas phase reactions were found over 1 wt.-% Pd/Siral70 catalyst under the following conditions: $m_{\text{Cat.}}$: 3 g, T: 380 °C, reactant feed: 5.1 g/h OA and 104.4 mL/min H_2. Similar results were obtained using Siral 40 and Siral 80 as support, but thereby more high boiling unidentified compounds in the boiling range between 280 °C and 320 °C were formed in comparison with the results obtained in the presence of the Siral 70 based catalyst. The addition of steam to the reaction lowered the product selectivity. No positive effect could be found.

Liquid phase reactions in the trickle bed reactor under atmospheric pressure showed the same liquid product yields and selectivities like the gas phase reaction in the plug flow fixed bed reactor. Raising the reaction pressure improved the product selectivity (up to 90%) enormously and reduced the formation of unsaturated hydrocarbons, especially of heptadecene. Unfortunately, it was not possible to run the gas phase reaction under elevated hydrogen pressure. Therefore, it is also possible to perform such gas phase reactions with similar results as the liquid phase reactions.

The best overall result was obtained with 1 wt.-% Pd/Siral70 as catalyst, a reaction temperature of 350 °C, a WHSV of 1.85 s^{-1} and a H_2 pressure of 15 bar. A distillation according to DIN 51 751 proved that conventional diesel and the product mixture obtained under these conditions have the same start- and end point of distillation and differs only in the hydrocarbon distribution.

By using the side products of the oil production (mixture of free fatty acids and tri-, di- and monoglycerides as well as mixtures with palm oil) the product selectivities obtained were slightly lowered because the contaminations in the feed leads to partial deactivation of the catalysts.

Acknowledgement

We gratefully acknowledge some financial support by ADM Research GmbH, Hamburg, Germanyand the permission to publish this work.

References

[1] U. Rashid, F. Anwar, Fuel 87 (2008) 265–273.
[2] B.M.E. Russbueldt, W.F. Hoelderich, J. Catal. 271 (2010) 290–304.
[3] G. Knothe, Fuel Process. Technol. 86 (2005) 1059–1070.
[4] Directive 2003/30/EC of the European Parliament and the council of 8 May 2003.
[5] K.G. Cassman, A.J. Liska, Bioprod. Biorefin. 1 (2007) 18–23.
[6] M.B. Charles, R. Ryan, N. Ryan, R. Oloruntoba, Energy Policy 35 (2007) 5737–5746.
[7] W.T. Coyle, A Report from the Economic Research Service, Next-Generation Biodiesel, United States Department of Agriculture, 2010.
[8] A. Vogel, F. Mueller-Langer, M. Kaltschmitt, Chem. Eng. Technol. 31 (2008) 755–764.
[9] S.N. Naik, V.V. Goud, P.K. Rout, A.K. Dalai, Renewable Sustainable Energy Rev. 14 (2010) 578–597.

[10] T. Kalnes, Int. J. Chem. Reactor Eng. 5 (2007) A48.
[11] http://www.nesteoil.com/default.asp?path=1,41,11991,22708,22721
[12] http://www.petrobras.com.br/en/our-activities/performance-areas/biofuel-production/
[13] http://www.uop.com/processing-solutions/biofuels/green-diesel/#green-diesel-production
[14] http://www.volkswagenag.com/content/vwcorp/info_center/en/publications/2004/09/SunFuel_Life_Cycle_Assessment.-bin.acq/qual-BinaryStorageItem.Single.File/sunfuel_english.pdf
[15] A. Bauen, in: C.J. Cleveland (Ed.), Encyclopedia of Energy, Vol. 1, Elsevier, 2004.
[16] J.R. Rostrup-Nielsen, Science 308 (2005) 1421–1422.
[17] K.H. Keim, Erdol & Kohle Erdgas Petrochemie 37 (12) (1984) 558–562.
[18] A.N.R. Bos, P.J.J. Tromp, H.N. Akse, Ind. Eng. Chem. Res. 34 (11) (1995) 3808–3816.
[19] E. Laurent, B. Delmon, Appl. Catal. A 109 (1994) 77–96.
[20] G.W. Huber, P. O'Connor, A. Corma, Appl. Catal. A 329 (2007) 120–129.
[21] O.İ. Şenol, E.-M. Ryymin, T.-R. Viljava, A.O.I. Krause, J. Mol. Catal. A Chem. 268 (2007) 1–8.
[22] M. Krár, S. Kovács, D. Kalló, J. Hancsók, Bioresour. Technol. 101 (2010) 9287–9293.
[23] M. Snåre, I. Kubickova, P. Mäki-Arvela, K. Eränen, D.Y. Murzin, Ind. Eng. Chem. Res. 45 (2006) 5708–5715.
[24] I. Simakova, O. Simakova, P. Mäki-Arvela, D.Y. Murzin, Catal. Today 150 (2010) 28–31.
[25] I. Simakova, O. Simakova, P. Mäki-Arvela, A. Simakov, M. Estrada, D.Y. Murzin, Appl. Catal. A 335 (2009) 100–108.
[26] S. Lestari, P. Mäki-Arvela, K. Eränen, J. Beltramini, G.Q. Max Lu, D.Y. Murzin, Catal. Lett. 134 (2010) 250–257.
[27] J.G. Immer, M.J. Kelly, H.H. Lamb, Appl. Catal. A 375 (2010) 134–139.
[28] M. Snåre, I. Kubičková, P. Mäki-Arvela, D. Chichova, K. Eränen, D.Y. Murzin, Fuel 87 (2008) 933–945.
[29] S. Lestari, P. Mäki-Arvela, H. Bernas, O. Simakova, R. Sjönholm, J. Beltrami, G.Q.M. Lu, J. Myllyoja, I. Simakova, D.Y. Murzin, Energy Fuels 23 (2009) 3842–3845.
[30] M. Arend, T. Nonnen, W.F. Hoelderich, J. Groos, J. Fischer, Appl. Catal.A 399 (2011) 198–204.
[31] F.A. Twaiq, N.A.M. Zabidi, S. Bhatia, Ind. Eng. Chem. Res. 38 (1999) 3230–3237.
[32] S.P.R. Katikaneni, J.D. Adjaye, N.N. Bakhshi, Can. J. Chem. Eng. 73 (1995) 484–497.
[33] X. Dupain, D.J. Costa, C.J. Schaverien, M. Makkee, J.A. Moulijn, Appl. Catal. B 72 (2007) 44–61.
[34] A. Corma, G.W. Huber, L. Sauvanaud, P. O'Connor, J. Catal. 247 (2007) 307–327.
[35] M. Breysse, P. Afanasiev, C. Geantet, M. Vrinat, Catal. Today 86 (2003) 5–16.
[36] D. Kubička, M. Bejblová, J. Vlk, Top. Catal. 53 (2010) 168–178.
[37] S.P.R. Katikaneni, J.D. Adjaye, R.O. Idem, N.N. Bakhshi, Ind. Eng. Chem. Res. 35 (1996) 3332–3346.
[38] J. Čejka, S. Minetova, Catal. Rev. Sci. Eng. 49 (2007) 457–509.
[39] Y.S. Ooi, R. Zakaria, A.R. Mohamed, S. Bhatia, Energy Fuel 18 (2004) 1555–1561.
[40] Y.S. Ooi, R. Zakaria, A.R. Mohamed, S. Bhatia, Energy Fuel 19 (2005) 736–743.
[41] C.L. Thomas, Ind. Eng. Chem. 41 (1949) 2564–2573.
[42] J. Hagen, Technische Katalyse, Wiley-VCH, Weinheim, 1996.
[43] W. Daniell, U. Schubert, R. Glöckler, A. Meyer, K. Noweck, H. Knörzinger, Appl. Catal. A 196 (2000) 247–260.